Clinical Radiology 74 (2019) 95–110

Contents lists available at ScienceDirect

Clinical Radiology

journal homepage: www.clinicalradiologyonline.net

Pictorial Review

The clinical significance of incidental soft tissue uptake on whole body ^{18}F-sodium fluoride bone PET-CT

S. Usmani [a,*], G. Gnanasegaran [b], F. Marafi [c], A. Esmail [c], N. Ahmed [d], T. Van den Wyngaert [e]

[a] Department of Nuclear Medicine, Kuwait Cancer Control Centre, Kuwait
[b] Royal Free Hospital NHS Trust, London, UK
[c] Jaber Al-Ahmad Molecular Imaging Center, Kuwait
[d] Jack Brignall PET/CT Centre, Castle Hill Hospital, Cottingham, UK
[e] Antwerp University Hospital, Antwerp, Belgium

ARTICLE INFORMATION

Article history:
Received 9 June 2018
Received in revised form
19 September 2018
Accepted 19 September 2018

^{18}F-sodium fluoride (NaF) is a PET bone imaging agent and is commonly used in imaging patients with cancer; however, similar to technetium-99m medronic acid (^{99m}Tc-MDP), it can be useful in the evaluation of benign bone and joint conditions. NaF is an excellent bone-seeking agent with high bone uptake due to rapid single-pass extraction. It has negligible plasma protein binding, rapid blood, renal clearance, high bone uptake and almost all NaF delivered is retained by bone after a single pass of blood; however, uptake of NaF can be observed in non-osseous structures such as the arterial vasculature, gastrointestinal tract, genitourinary tract, and viscera. In this article, we present a spectrum of clinical cases with non-osseous NaF uptake in patients referred for cancer staging.

© 2018 The Royal College of Radiologists. Published by Elsevier Ltd. All rights reserved.

Introduction

Sodium fluoride-18 (^{18}F-NaF) is an excellent bone-seeking agent owing to high bone uptake due to rapid single-pass extraction, minimal binding to serum proteins, and fast clearance from the soft tissues.[1] It is a sensitive tool for detecting skeletal metastases in adults and it surpasses conventional bone scintigraphy.[2,3] Encouraging results have also been reported for its use in characterising benign bone disease in young patients.[4,5]

^{18}F-NaF positron-emission tomography (PET) combined with computed tomography (CT) improves diagnostic confidence with definitive reports in the majority of the cases with a high inter-rater agreement.[6] This superior diagnostic profile must be attributed to improved signal-to-noise ratio due to better bone accumulation versus soft-tissue dissemination and the higher spatial resolution.[7] In general, ^{18}F-NaF PET-CT has better delineation and anatomical localisation of bony lesions; however, non-osseous uptake of ^{18}F-NaF can sometimes be observed in structures such as the arterial vasculature, gastrointestinal tract, genitourinary tract, and other organ systems.[8] In hybrid imaging,

* Guarantor and correspondent: S. Usmani, Department of Nuclear Medicine, Kuwait Cancer Control Center, PO Box: 1488, 83001 Khaitan, Kuwait. Tel.: +96597613437.
E-mail address: dr_shajji@yahoo.com (S. Usmani).

https://doi.org/10.1016/j.crad.2018.09.007
0009-9260/© 2018 The Royal College of Radiologists. Published by Elsevier Ltd. All rights reserved.

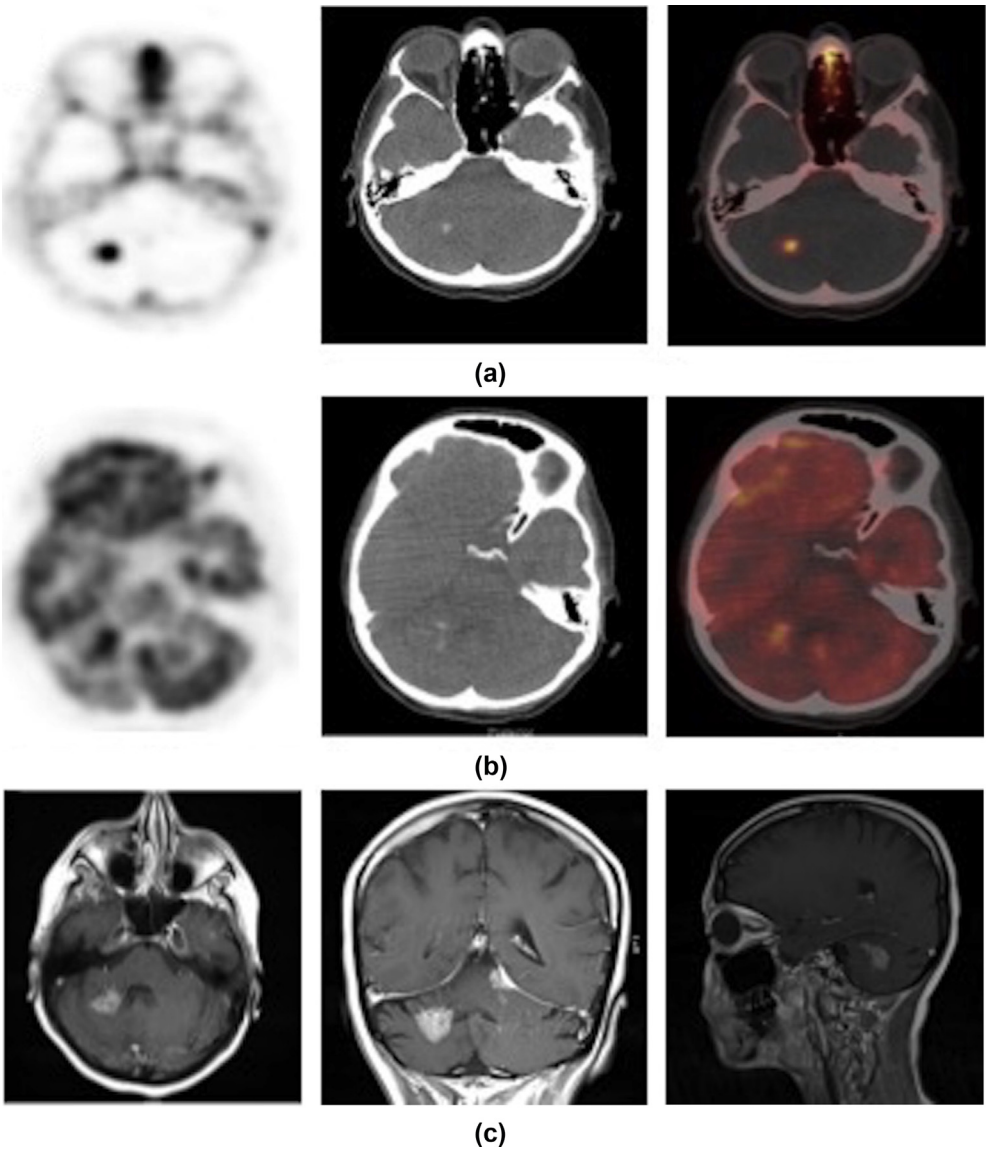

Figure 1 Brain. A 45-year-old woman with metastatic breast cancer, complained of back pain. ^{18}F-NaF-PET-CT was performed to rule out bone metastasis. (a) Cross-sectional NaF images show focal increased NaF uptake in the right cerebellum. The corresponding unenhanced CT image shows calcification and increased tracer uptake on the fused images. (b) ^{18}F-FDG PET-CT images show congruent hypermetabolic lesion in the right cerebellum. (c) MRI confirmed solitary cerebellar metastasis (high intensity signal lesion). No sinister cause for the back pain was identified.

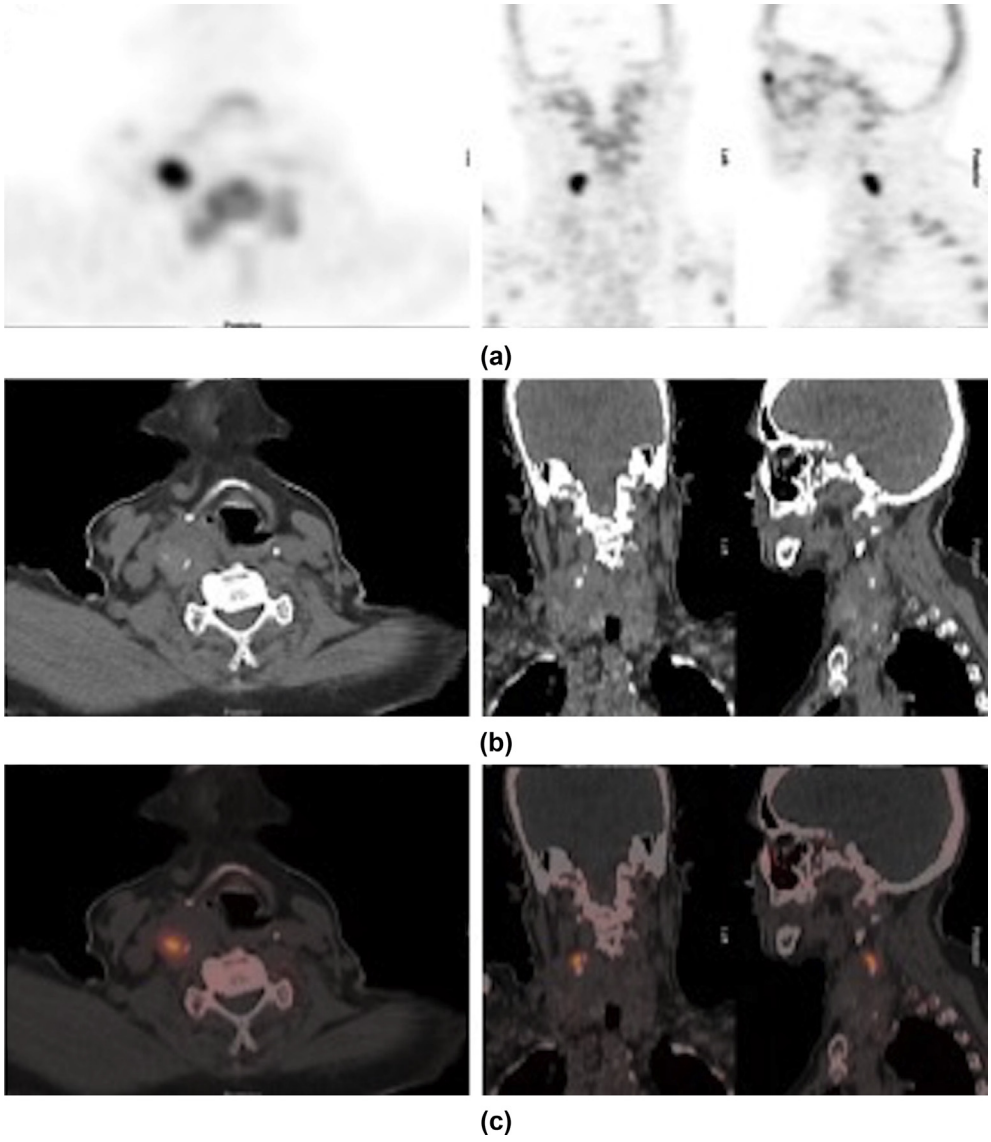

Figure 2 Thyroid. A 81-year-old woman with breast cancer presented with back pain. (a) ^{18}F-NaF images show increased tracer uptake at right side of the neck. (b–c) Unenhanced CT and fused PET-CT images show a calcified thyroid nodule with corresponding increased tracer uptake. Fine-needle aspiration cytology (FNAC) of the thyroid nodule confirmed papillary thyroid cancer.

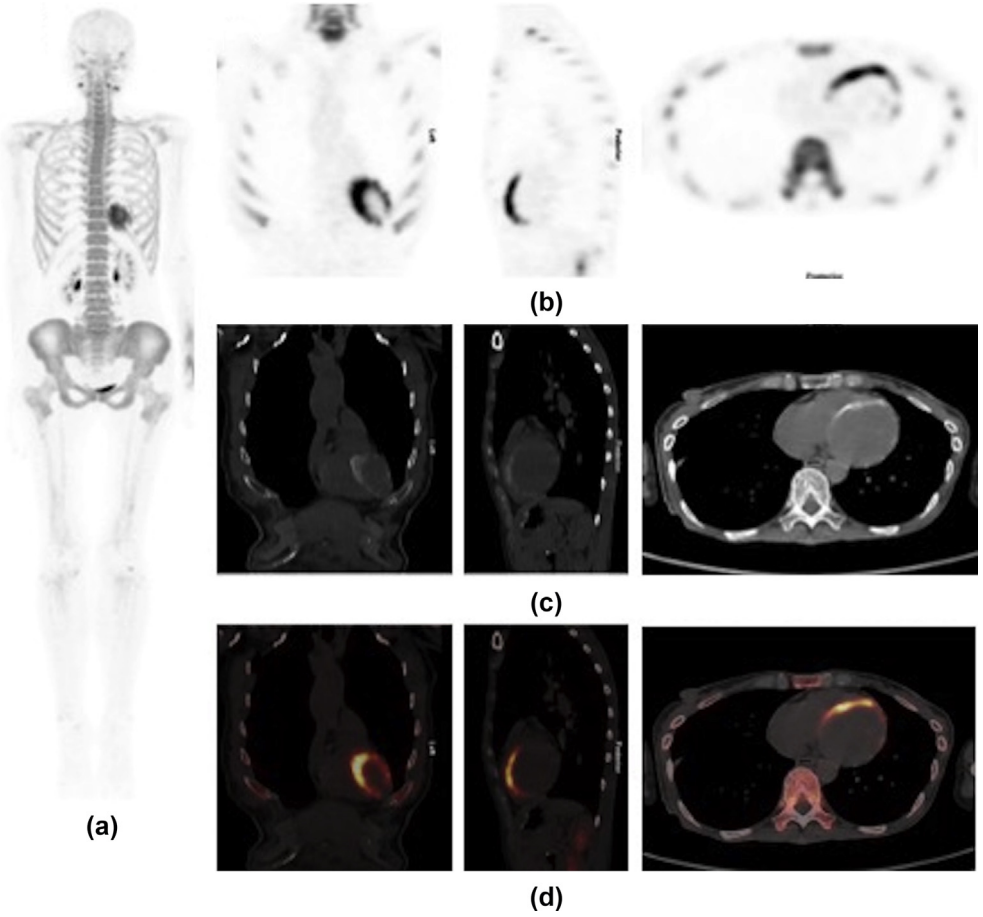

Figure 3 Cardiac. A 48-year-old woman with gastric cancer underwent total gastrectomy 2 years previously. Patient complained of generalised bone pain. (a) Whole-body maximum intensity projection (MIP) image shows soft-tissue uptake within left hemi-thorax. (b–d) ^{18}F-NaF PET-CT images show increased tracer uptake within a calcified left ventricular wall. There was neither an established history of myocarditis nor that of an ischaemic event. The findings most likely represent myocardial calcification related to a dystrophic or an idiopathic cause.

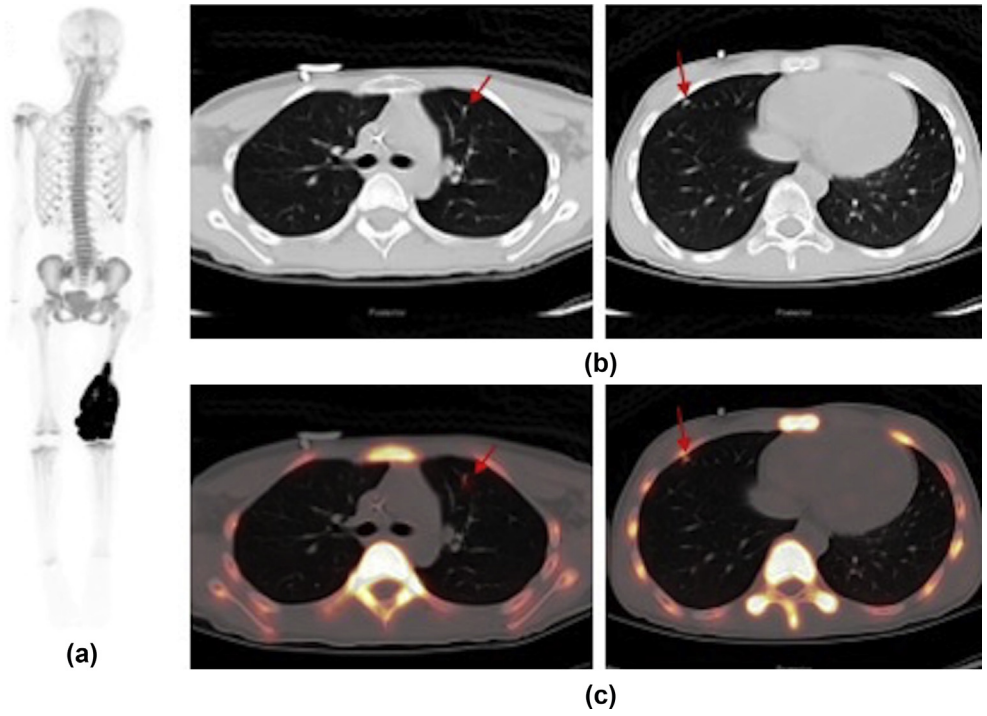

Figure 4 Lung. An 11-year-old female patient with osteosarcoma of the distal left femur in which ^{18}F-NaF-PET-CT was performed for staging. (a) Anterior MIP images show increased tracer uptake in the distal half of the left femur at the primary tumour site. No other distant skeletal lesion was seen. (b–c) CT and fused PET-CT images show two small pulmonary nodules, which demonstrate faint activity. The faint activity is likely reflective of the size of these nodules. These nodules were later confirmed as metastases on follow-up high-resolution CT.

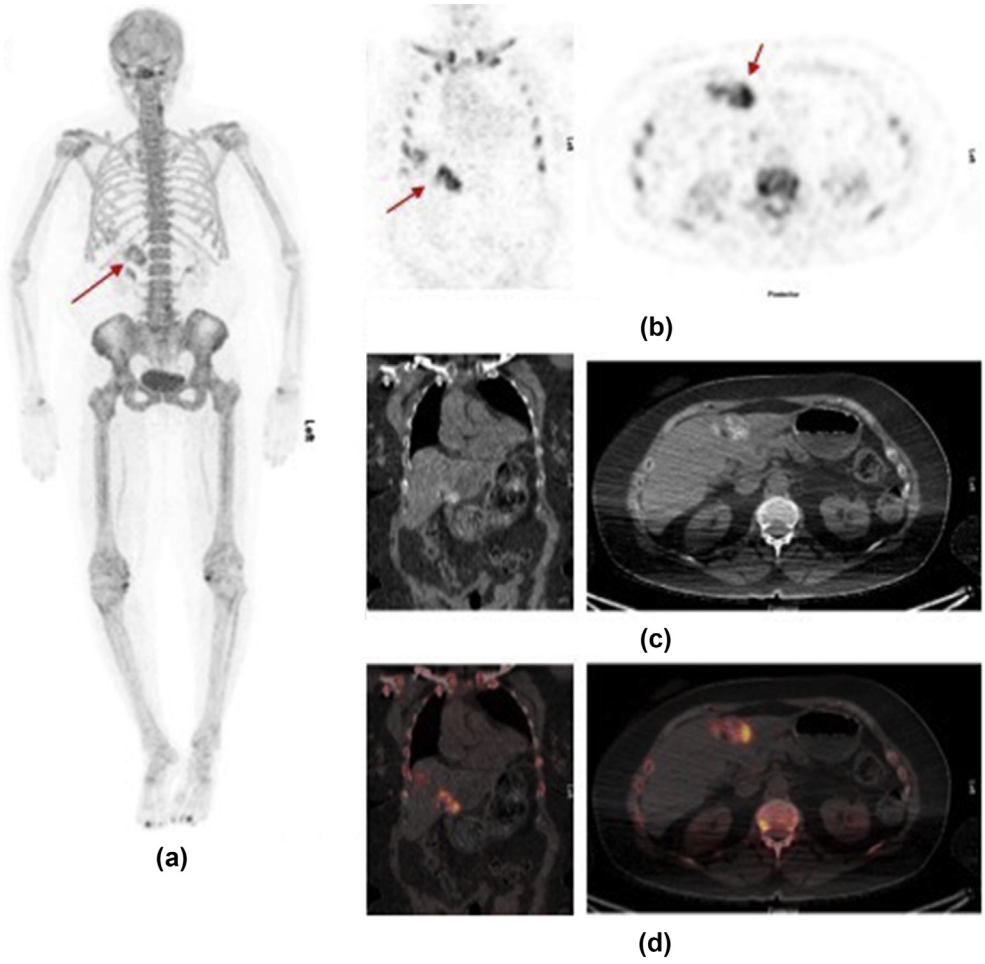

Figure 5 Liver. A 66-year-old woman with metastatic colon cancer. The patient complained of generalised bone pain. (a) ^{18}F-NaF MIP images show increased tracer uptake in the right hypochondrial region (arrow). (b) Transaxial and coronal NaF images show increased tracer uptake within the left lobe of the liver. (c–d) Unenhanced CT and fused PET-CT images show uptake in calcified hepatic lesions consistent with known liver metastases.

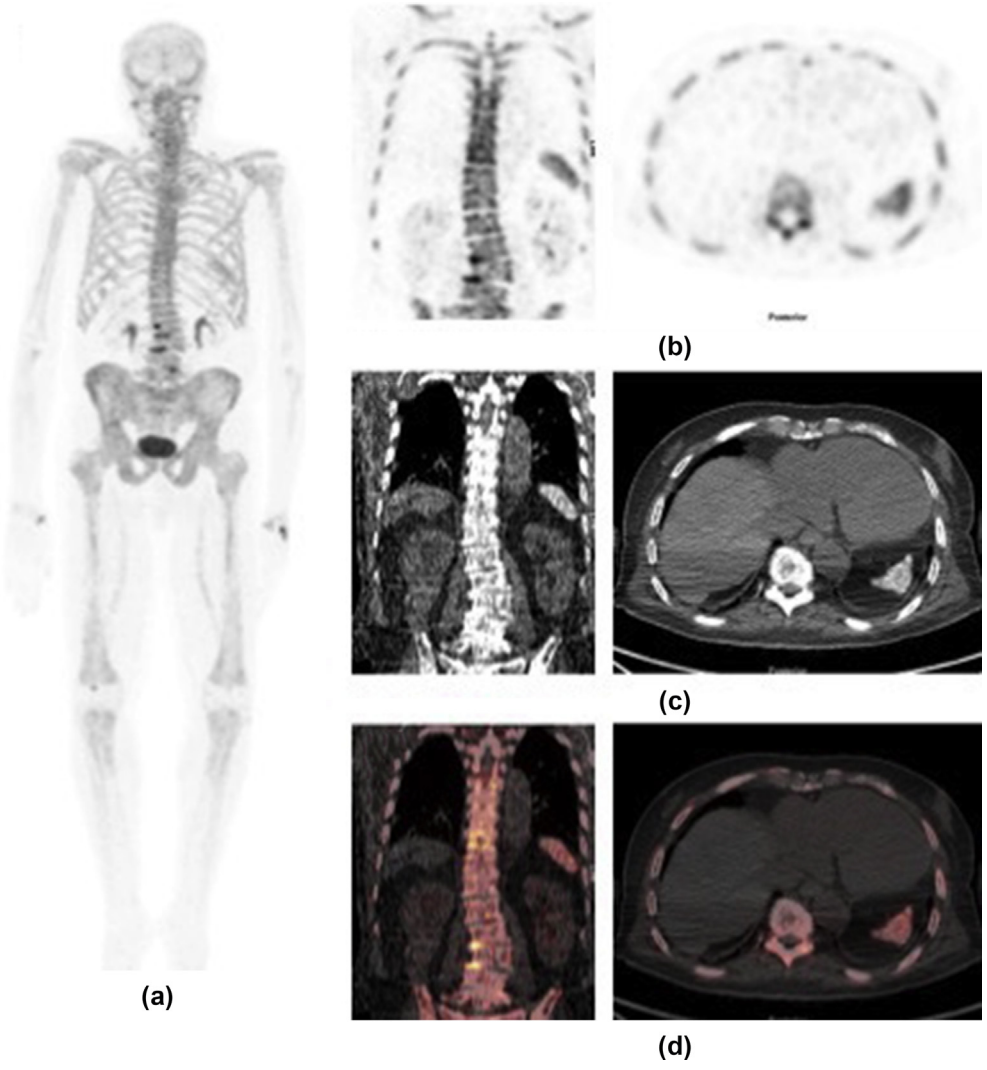

Figure 6 Spleen. A 76-year-old man with prostate cancer and sickle cell disease complained of low back pain. His PSA was 0.02 ng/ml. (a) ^{18}F-NaF MIP images show the scoliotic lumbar spine with increased tracer uptake at the endplates and facet joints of L3–L5 vertebrae in keeping with degenerative changes. (b–d) Increased NaF uptake is noted in the left hypochondrial region, corresponding on CT to an atrophic calcified spleen, compatible with splenic infarction secondary to sickle cell disease.

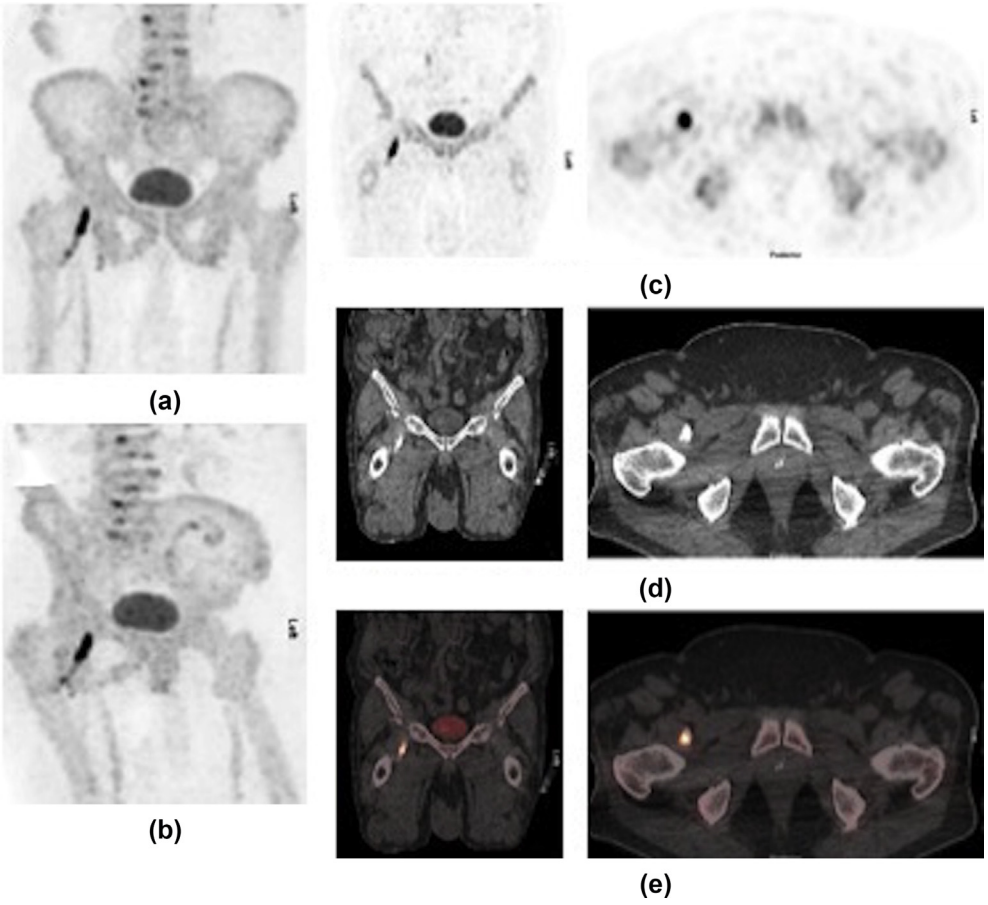

Figure 7 Muscle. An 84-year-old woman with breast cancer complained of right hip pain for which there was history of trauma 6 months previously. (a) Anterior (b) oblique ^{18}F-NaF MIP and (c) cross-sectional images demonstrate linear increased tracer uptake in the right groin, which corresponds to calcification within the iliopsoas muscle as seen on the unenhanced CT images (d) and corresponding fused ^{18}F-NaF PET-CT images (e). The findings are in keeping with myositis ossificans.

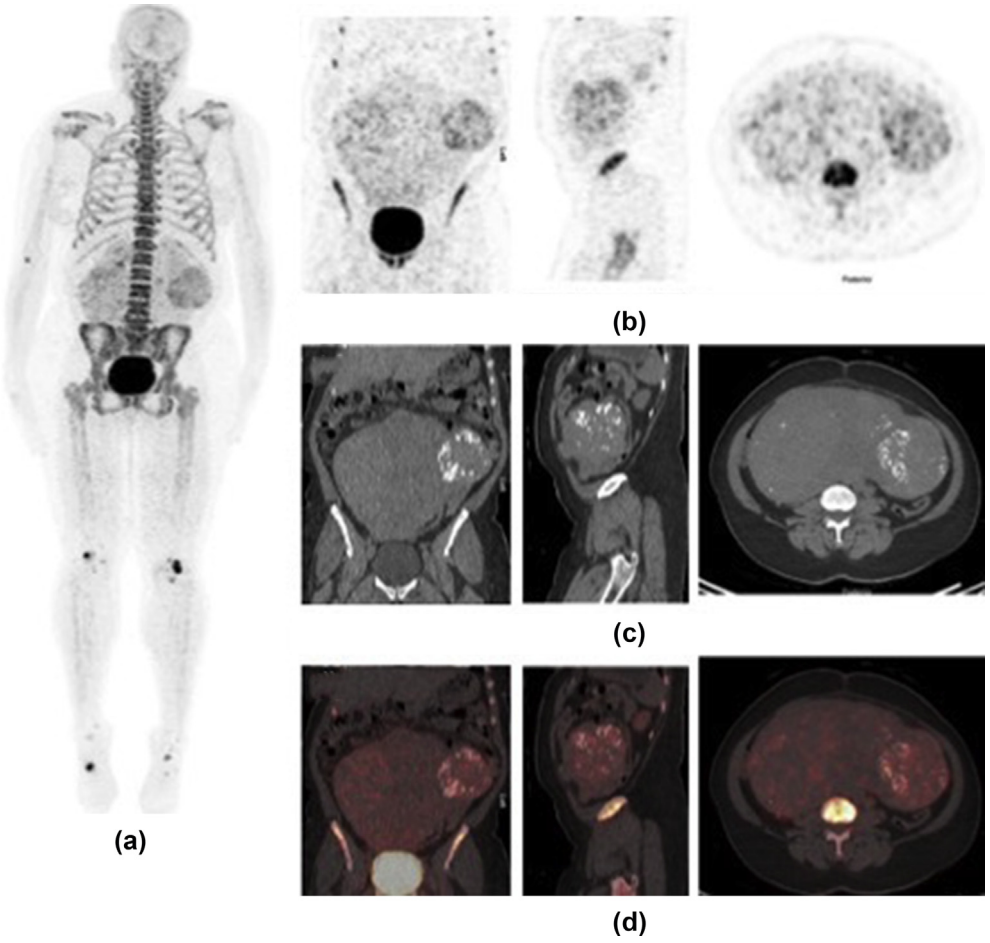

Figure 8 Abdominopelvic mass. A 52-year-old woman with breast cancer. (a) ^{18}F-NaF MIP images show diffuse abnormal soft-tissue uptake in the abdomen, more so on the left side. (b–d) Increased ^{18}F-NaF uptake corresponds to a large lobulate heterogeneous abdominopelvic mass with calcification. The large mixed cystic–solid mass was consistent with synchronous ovarian malignancy.

anatomical localisation with CT often improves both the specificity of assessment of the bone lesion and soft-tissue uptake. In general, ^{18}F-NaF bone scintigraphy is often used in cancer patients to detect the presence of any skeletal metastases. The interpretation is based on the pattern of tracer uptake in the bones, which is often identified as areas of increased tracer uptake (focal or diffuse) and occasionally as areas of decreased or absent uptake within a bone. Extra-osseous ^{18}F-NaF uptake can be seen similar to technetium-99m medronic acid (^{99m}Tc-MDP).[9] In this review, we present a spectrum of cases with extra-osseous ^{18}F-NaF uptake, identified as an incidental finding on patients referred for staging cancers.

^{18}F-NaF PET CT acquisition protocol

Images were acquired after intravenous injection of 2.2 MBq/kg ^{18}F-NaF with a 60–90 minute uptake period.[10,11] PET emission images were obtained in a three-dimensional mode at 2–3 minutes per bed position according to patient BMI (2 minutes for BMI $<$35 kg/m^2; 2.5 minutes (35–39.9 kg/m^2), and 3 minutes for BMI $>$40 kg/m^2) from vertex to toes and reconstructed with a standard iterative algorithm (ordered-subset expectation maximisation, 3 iterative steps and 32 subsets) and filter cut-off of 6.4 mm as recommended by the manufacturer. Unenhanced CT was performed using an automatic tube current of 50–120 mA as determined by an automated algorithm based on the planar view to achieving a noise index of 20, 120 kVp, and pitch of 1.3. The CT axial images were reconstructed in a 512$\times$512 matrix, with a thickness of 3.75 mm. The radiation dosimetry for an ^{18}F-NaF PET is similar to ^{99m}Tc-MDP imaging, and optimal high-quality ^{18}F-NaF imaging can be performed effectively using a relatively smaller administered activity than is typically administered for ^{99m}Tc-MDP bone scintigraphy, resulting in an actual radiation absorbed dose equivalent to that of single-photon emission CT (SPECT) bone scintigraphy.[11] The effective dose imparted by ^{18}F-NaF (internal exposure) has been calculated by using coefficient 0.089 mrem/mCi (0.024 mSv/MBq) according to ICRP publication 106.[12] Recently published data by our group[13] showed that optimal high-quality bone scintigraphy in an adult can be achieved with

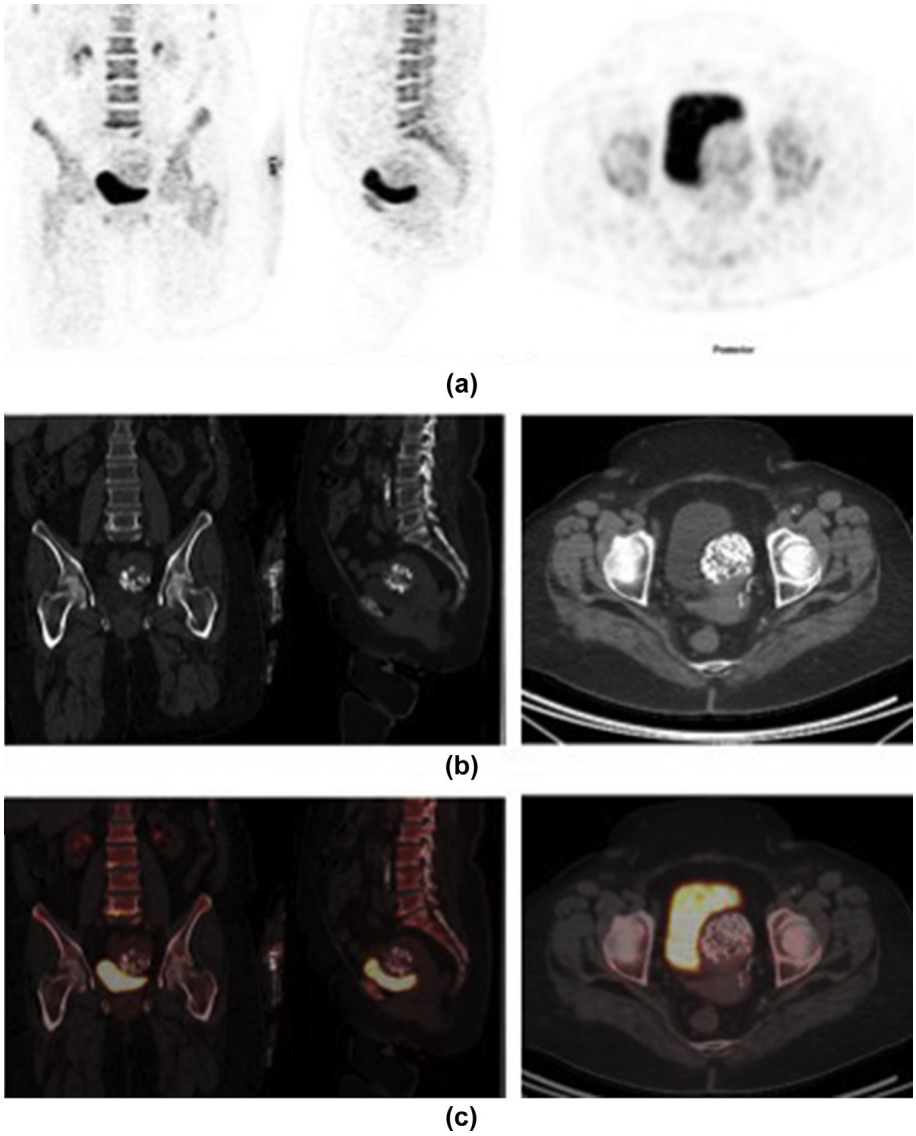

Figure 9 Uterus. An 85-year-old woman with breast cancer and back pain. (a) ^{18}F-NaF PET-CT images show a mass impressing on the urinary bladder on the left side, which corresponds to a calcified uterine fibroid on CT demonstrating mild heterogeneous tracer uptake similar to the pelvic bones.

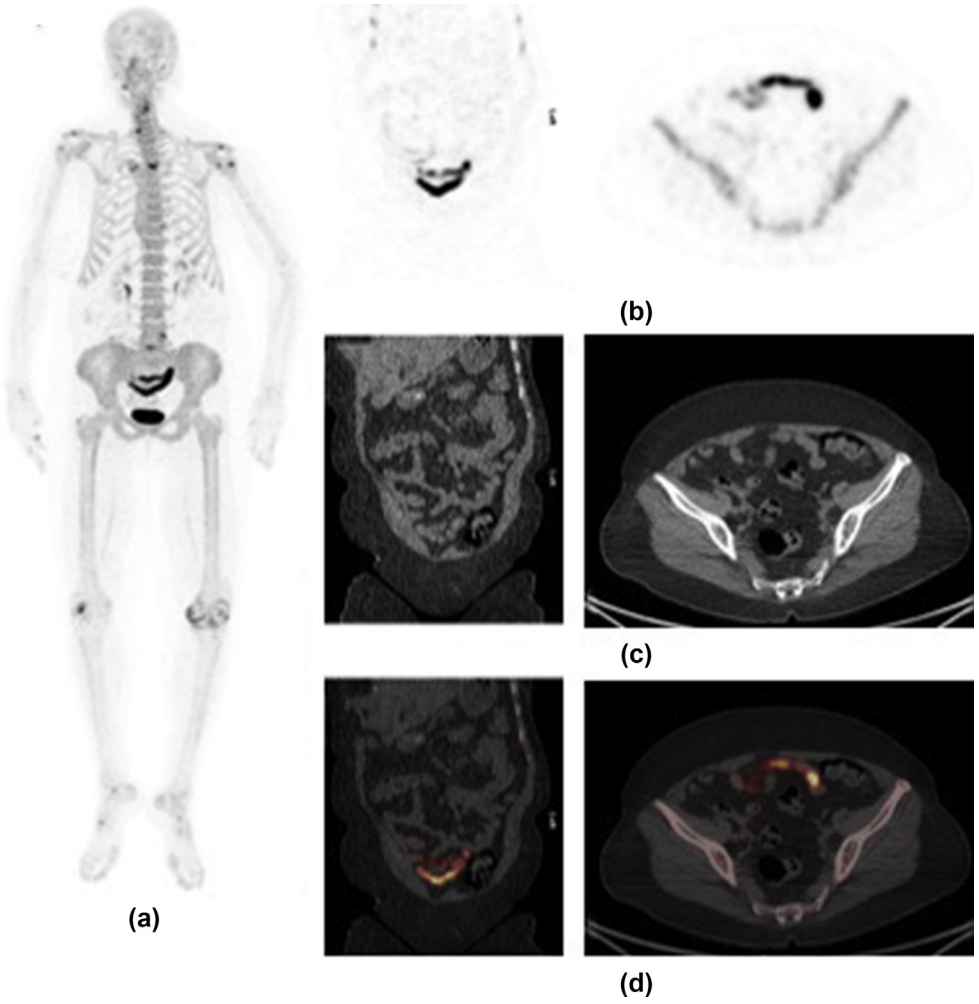

Figure 10 Bowel. A 59-year-old woman with breast cancer. (a) ^{18}F-NaF MIP images show increased tracer uptake in both acromioclavicular, sternoclavicular, knee joints and endplates of L5/S1 vertebrae in keeping with degenerative changes. (b) There is curvilinear increased tracer uptake seen in the pelvic region, which localises to the small bowel loops on PET-CT images (c–d). This pattern of activity has been described with non-specific physiological uptake in the small bowel of unknown significance. The other possible causes of similar pattern of uptake is active colitis or neoplasia; however, in the absence of any morphological abnormality on CT and any relevant clinical features, this is unlikely to represent synchronous pathology and therefore considered idiopathic in this case.

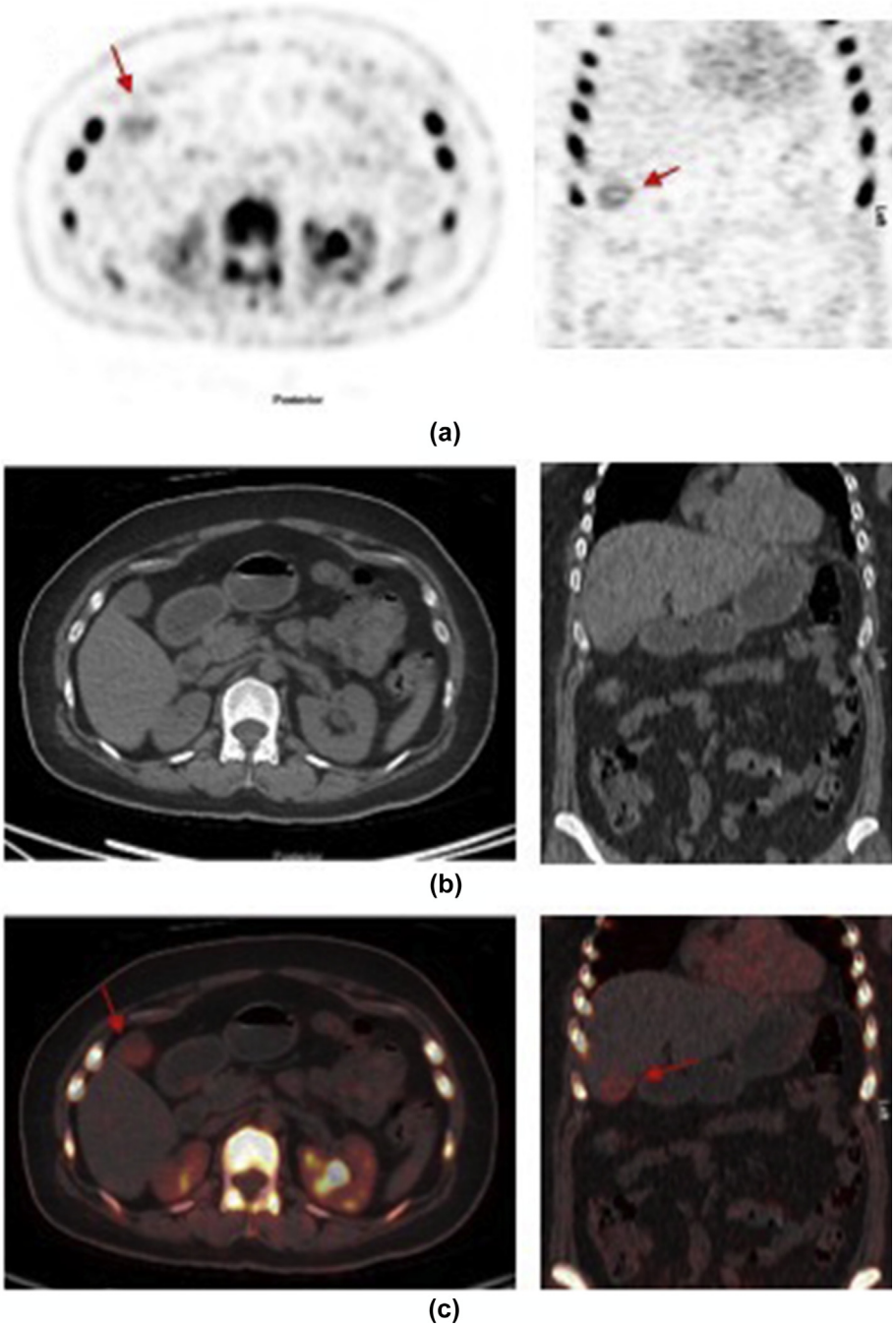

Figure 11 Gallbladder. A 74-year-old woman with breast cancer. (a–c) ^{18}F-NaF PET-CT images show mild increase tracer localisation within the right hypochondrium, which corresponds to gallbladder on the CT. The differentials include physiological hepatobiliary clearance or possibly increased vascularity secondary to low-grade infection or inflammation. Ultrasonography did not show any focal lesion in the wall of the gall bladder nor any gallstones.

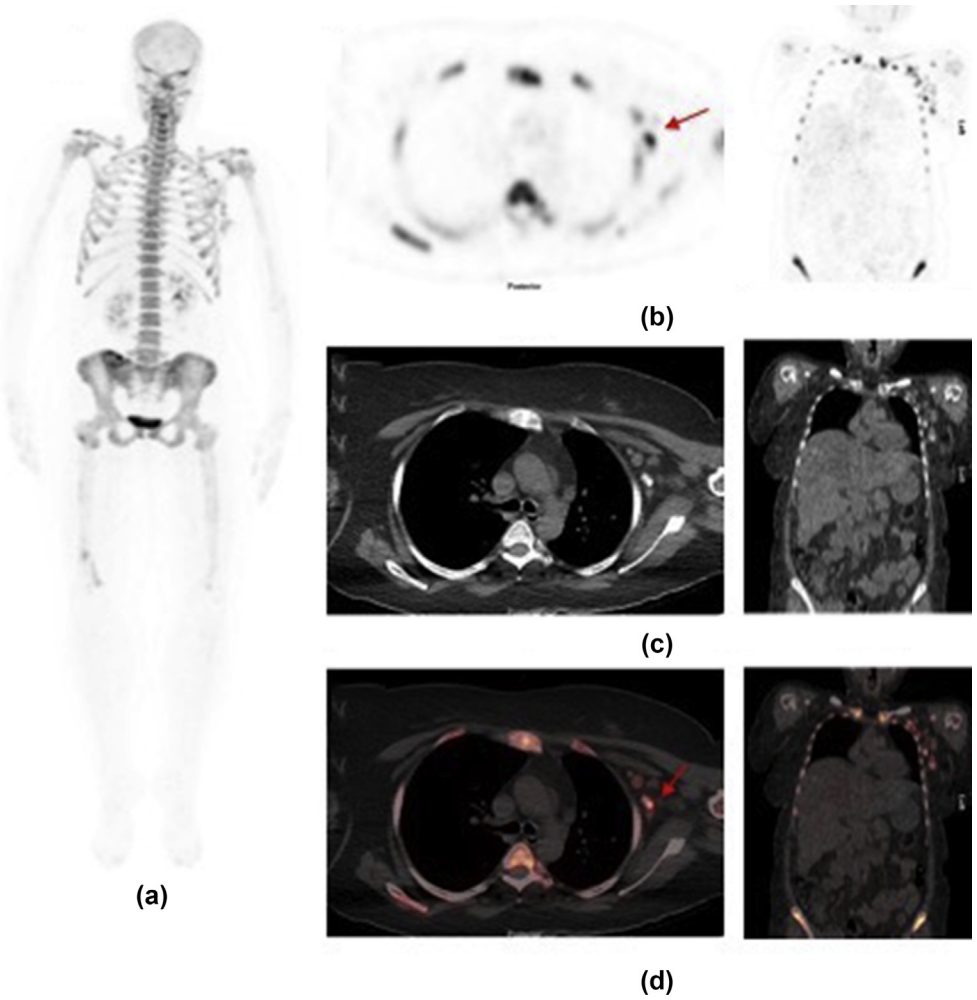

Figure 12 Lymph node. A 38-year-old woman with left breast cancer. (a) ^{18}F-NaF MIP images show increase tracer at right iliac bone and distal right femur highly suspicious for bone metastases. Some focal uptake near the right greater trochanter with no corresponding focal bone lesion likely of benign relevance for example to enthesopathy (b) Transaxial and coronal NaF images show increase tracer uptake within multiple left axillary lymph nodes. (c) Unenhanced CT images show multiple enlarged left axillary lymph nodes with calcification and corresponding increased uptake on fused images (d). Biopsy confirmed lymph node metastases. Both benign and malignant calcified nodes can take up ^{18}F-NaF.

injected activity as low as 0.06 mCi/kg of ^{18}F-NaF. The total effective dose of ^{18}F-NaF PET with low-dose CT is approximately 8.8±1.8 mSv, compared to approximately 7.4 mSv for bone SPECT/CT.[10]

Pharmacokinetics and mechanism of uptake

^{18}F-NaF bone uptake is related to blood flow and almost all ^{18}F-NaF delivered is retained by bone after a single pass of blood, resulting in an almost 100% first-pass extraction.[14] The bone uptake of ^{18}F-NaF is double that of ^{99m}Tc-MDP.[15] Uptake of NaF has a similar mechanism compared to ^{99m}Tc-MDP: following chemisorption of fluoride ions onto the surface of hydroxyapatite, they exchange with the hydroxyl (OH^-) ions in the crystal, forming fluorapatite.[9] It has negligible plasma protein binding, rapid blood and renal clearance, and high bone uptake early after injection, which is reflected in high target-to-background ratios.[1] Approximately 30% of the injected dose is found in the red blood cells, which does not interfere with bone uptake, as ^{18}F-NaF freely diffuses across the cell membrane. Plasma clearance is very rapid. Approximately 50% of the injected ^{18}F-NaF is taken up in bone.[16]

Extra-osseous uptake of ^{18}F-NaF

^{18}F-NaF is a bone imaging agent, but often variable tracer uptake in the soft tissues is observed, such as the arterial vasculature, genitourinary tract, and occasionally, in the gastrointestinal tract. As a bone-seeking agent, ^{18}F-NaF might also localise in extra-osseous calcifying lesions.[17] Lesions containing dystrophic or microscopic calcification, or calcified visceral metastases can show focal increased uptake of ^{18}F-NaF. Soft-tissue calcifications secondary to tumoural necrosis, vascular, infectious, or traumatic process often demonstrate ^{18}F-NaF uptake. In general, recognition of such findings might be of diagnostic value in occasional cases. The mechanisms of uptake of ^{18}F-NaF in the soft tissue are reported to be similar to ^{99m}Tc-MDP bone

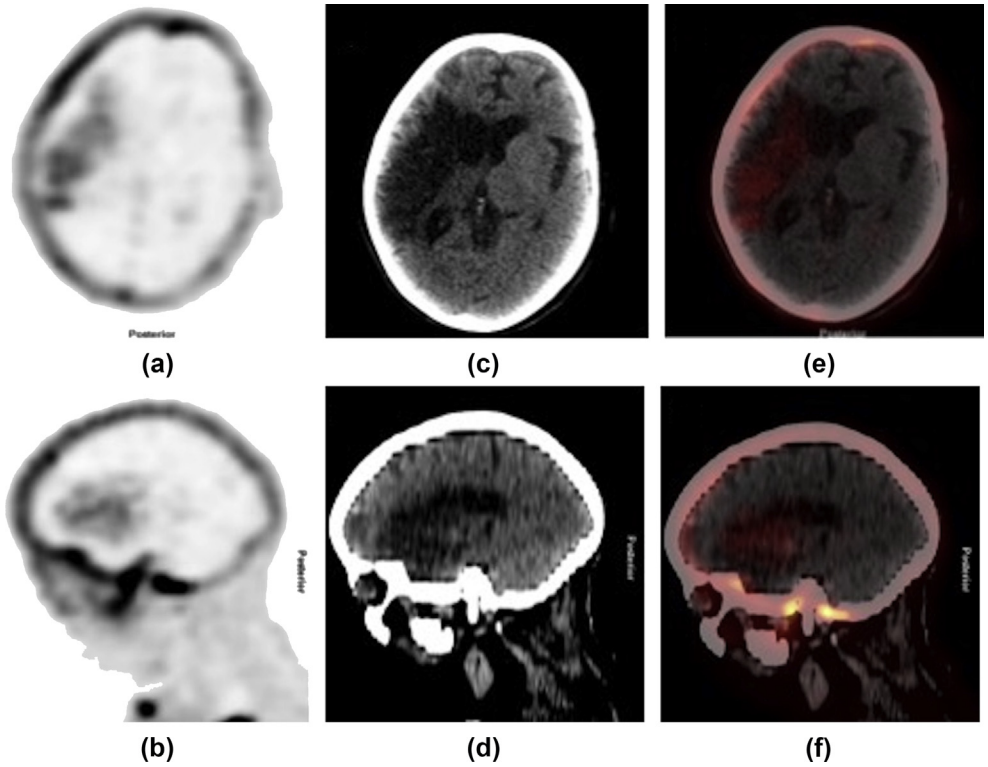

Figure 13 Cerebral infarct. A 79-year-old woman recently diagnosed with breast cancer was referred for ^{18}F-NaF PET-CT staging. The patient had a history of left hemiplegia due to cerebral infarct 20 months previously. (a,b) ^{18}F-NaF images show mild heterogeneously increased tracer localisation within the right parieto-temporal region corresponding to a hypodense area on unenhanced CT (c,d) with increased ^{18}F-NaF uptake on corresponding fused images (e,f). Findings are compatible with an increased ^{18}F-NaF uptake at the old infarct.

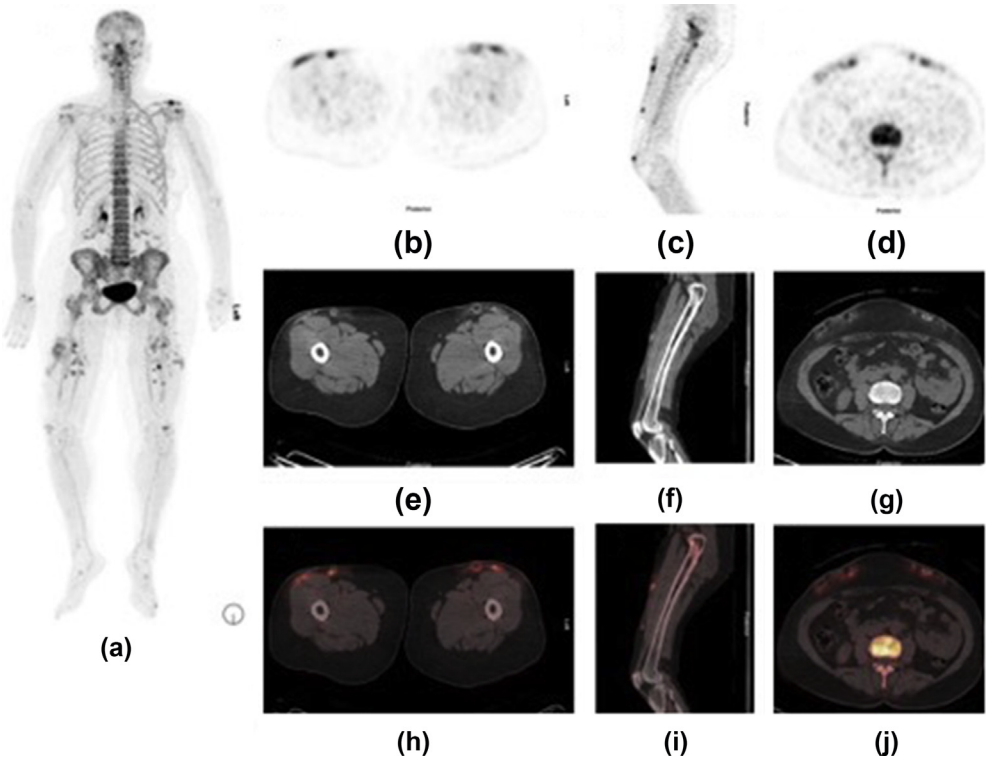

Figure 14 Subcutaneous calcification. A 64-year-old diabetic woman with breast cancer. (a) ^{18}F-NaF MIP images show increased tracer uptake in the anterior abdominal wall and thigh region. ^{18}F-NaF uptake is also seen in the left acromioclavicular, bilateral knee joints, and L5/S1 vertebral endplates suggestive of degenerative changes. (b–d) There is heterogeneous increased uptake in the subcutaneous soft tissues within the bilateral thighs and anterior abdominal wall. (e–g) Unenhanced CT images show subcutaneous calcifications and corresponding increased uptake on fused images (h–j). Multiple subcutaneous calcifications with osteoblastic activity are secondary to subcutaneous injection granulomas.

scintigraphy. The reported mechanisms include (a) local tissue necrosis or damage leading to increased calcium deposition in the tissue, (b) hyperaemia, (c) altered capillary permeability, (d) adsorption onto tissue calcium, (e) presence of iron deposits, and (f) binding to enzyme receptors or denatured proteins.[18]

In this review, we provide illustrated examples of extra-skeletal ^{18}F-NaF localisation due to both benign and malignant conditions (Figs 1–14). Malignant primary or metastatic lesions can accumulate ^{18}F-NaF because of tumour calcification or calcifications within the necrosis (Figs 1, 2, 4, 5, 8, 9 and 12). ^{18}F-NaF localisation in benign causes includes subcutaneous/muscle calcification (Figs 7 and 14), ischaemic/infarcted tissue (Figs 3, 6 and 13), and due to variable clearance of the tracer (Figs 10 and 11).

In the literature, several case reports have been reported for both malignant and benign aetiologies (Table 1). The tracer uptake in malignant aetiologies include brain metastasis,[19,20] cardiac metastasis[21] lymph nodes,[22] liver,[23,24] and ovarian metastasis.[25] The tracer uptake in benign causes include cardiac amyloidosis,[26] meningioma,[27] lung amyloidosis,[28] atherosclerosis,[29] and injection-related subcutaneous calcification.[30] The mechanisms of extra-osseous ^{18}F-NaF uptake are not fully clarified; however, in general, any process that involves active calcium deposition can take up ^{18}F-NaF. The mechanism of ^{18}F-NaF uptake in calcified metastatic lesions is by its direct incorporation into the hydroxyapatite crystals.[31] In soft-tissue metastases, tumour necrosis might demonstrate ^{18}F-NaF avidity due to dystrophic calcification[17]; however, it is not clear how ^{18}F-NaF is taken up in non-calcified metastasis. Sheth *et al.*[22] reported ^{18}F-NaF uptake in metastatic lymph nodes, which might be related to the presence of microscopic calcifications; however, the true significance of ^{18}F-NaF uptake in the lymph nodes remains unknown. Recent studies have investigated ^{18}F-NaF PET as a marker of vascular calcification in aortic stenosis and atherosclerosis affecting the aorta, coronary, and carotid arteries.[29,32,33] In bone, ^{18}F-NaF is thought to incorporate onto the surface of hydroxyapatite crystals.[31] Given that hydroxyapatite is also a key component of vascular calcification, it is presumed to be the radiotracer target in aortic sclerosis and atherosclerosis.[34] Increased tracer uptake has also been described in a renal, ureteric, and bladder stones.[35,36] The possible explanation suggested is due to the accumulation of the radionuclide secondary to sluggish flow and its adsorption onto the crystal surface within the calculi.[37,38]

Table 1
Overview of reports of extra osseous ^{18}F-NaF uptake.

Tissue origin	Classification	No. of reported cases [reference]
Brain	Metastases	4[19,20,39,40]
	Meningioma	1[27]
	Cerebral infarcts	1[41]
Cardiac	Metastases	1[21]
	Amyloidosis	1[26]
	Coronary calcification	4[29,32,42,43]
Liver	Metastases	5[23,24,44,45,49]
Lung	Non-small cell lung carcinoma	1[46]
	Metastases	1[47]
	Amyloidosis	1[28]
Lymph node	Metastases	2[22,49]
Ovary	Metastases	1[25]
Skin	Subcutaneous calcification	1[30]
Stomach	Hypercalcaemia	1[48]
Thyroid	Thyroid cancer	1[49]
Vessels	Atherosclerosis	4[29,33,34]
Urinary tract and bladder	Bladder stone	1[35]
	Urinary bladder cancer	1[50]

Conclusions

^{18}F-NaF PET-CT is an emerging and promising bone imaging agent for characterisation of osseous lesions; however, extra-osseous tracer uptake is not uncommon, and occasionally these non-osseous findings may alter diagnosis and subsequent management. The present review also highlights the overall similar spectrum of extra-osseous findings seen with ^{99m}Tc-MDP, and this established knowledge can translate into confident recognition of normal and abnormal extra-osseous ^{18}F-NaF uptake while reporting these scans in routine clinical practice.

Conflict of interest

The authors declare that they have no conflict of interest.

References

1. Czernin J, Satyamurthy N, Schiepers C. Molecular mechanisms of bone ^{18}F-NaF deposition. *J Nucl Med* 2010;**51**:1826–9.
2. Even-Sapir E, Metser U, Mishani E, *et al.* The detection of bone metastases in patients with high-risk prostate cancer: 99mTc-MDP planar bone scintigraphy, single- and multi-field-of-view SPECT, 18F-fluoride PET, and 18F-fluoride PET/CT. *J Nucl Med* 2006;**47**:287–97.
3. Löfgren J, Mortensen J, Rasmussen SH, *et al.* A prospective study comparing 99mTc-hydroxyethylene-diphosphonate planar bone scintigraphy and whole-body SPECT/CT with ^{18}F-fluoride PET/CT and ^{18}F-fluoride PET/MRI for diagnosing bone metastases. *J Nucl Med* 2017;**58**:1778–85.
4. Drubach LA, Sapp MV, Laffin S, *et al.* Fluorine-18 NaF PET imaging of child abuse. *Pediatr Radiol* 2008;**38**:776–9.
5. Laverick S, Bounds G, Wong WL. [18F]-Fluoride positron emission tomography for imaging condylar hyperplasia. *Br J Oral Maxillofac Surg* 2009;**47**:196–9.
6. Even-Sapir E, Metser U, Flusser G, *et al.* Assessment of malignant skeletal disease: initial experience with ^{18}F-fluoride PET/CT and comparison between ^{18}F-fluoride PET and ^{18}F-fluoride PET/CT. *J Nucl Med* 2004;**45**:272–8.
7. Grant FD, Fahey FH, Packard AB, *et al.* Skeletal PET with ^{18}F-fluoride: applying new technology to an old tracer. *J Nucl Med* 2008;**49**:68–78.
8. Derlin T, Tóth Z, Papp L, *et al.* Correlation of inflammation assessed by ^{18}F-FDG PET, active mineral deposition assessed by ^{18}F-fluoride PET, and vascular calcification in atherosclerotic plaque: a dual-tracer PET/CT study. *J Nucl Med* 2011;**52**:1020–7.
9. Fogelman I. Skeletal uptake of disphosphonate: a review. *Eur J Nucl Med Mol Imag* 1980;**5**:473–6.
10. Beheshti M, Mottaghy FM, Payche F, *et al.* ^{18}F-NaF PET/CT: EANM procedure guidelines for bone imaging. *Eur J Nucl Med Mol Imag* 2015;**42**:1767–77.
11. Segall G, Delbeke D, Stabin MG, *et al.* SNM practice guideline for sodium ^{18}F-fluoride PET/CT bone scans 1.0. *J Nucl Med* 2010;**51**:1813–20.
12. Radiation dose to patients from radiopharmaceuticals. Addendum 3 to ICRP publication 53. ICRP Publication 106. Approved by the Commission

in October 2007. Ann ICRP, 38, 1–197, http://www.bmap.ucla.edu/docs/ICRP_106_RadiationDosetoPatientsfromRadiopharmaceuticals_vol38_2008.pdf.
13. Marafi F, Esmail A, Rasheed R, *et al*. Novel weight-based dose threshold for ^{18}F-NaF PET-CT imaging using advanced PET-CT systems: a potential tool for reducing radiation burden. *Nucl Med Commun* 2017;**38**:764–70.
14. Frost ML, Blake GM, Cook GJ, *et al*. Differences in regional bone perfusion and turnover between lumbar spine and distal humerus: ^{18}F-fluoride PET study of treatment-naive and treated postmenopausal women. *Bone* 2009;**45**:942–8.
15. Blake GM, Park-Holohan SJ, Cook GJ, *et al*. Quantitative studies of bone with the use of ^{18}F-fluoride and ^{99m}Tc-methylene diphosphonate. *Semin Nucl Med* 2001;**31**:28–49.
16. Dworkin H, Moon N, Lessard R, *et al*. A study of the metabolism of fluorine-18 in dogs and its suitability for bone scanning. *J Nucl Med* 1966;**7**:510–20.
17. Stewart VL, Herling P, Dalinka MK. Calcification in soft tissues. *JAMA* 1983;**250**:78–81.
18. Gnanasegaran G, Cook G, Adamson K, *et al*. Patterns, variants, artifacts, and pitfalls in conventional radionuclide bone imaging and SPECT/CT. *Semin Nucl Med* 2009;**39**:380–95.
19. Wu J, Zhu H, Ji H. Unexpected detection of brain metastases by ^{18}F-NaF PET/CT in a patient with lung cancer. *Clin Nucl Med* 2013;**38**:e429–32.
20. Kuyumcu S, Adalet I, Isik EG, *et al*. Impact of nonosseous findings on ^{18}F-NaF PET/CT in a patient with ductal breast carcinoma. *Nucl Med Mol Imag* 2014;**48**:72–4.
21. Chou YH, Ko KY, Cheng MF, *et al*. ^{18}F-NaF PET/CT images of cardiac metastasis from osteosarcoma. *Clin Nucl Med* 2016;**41**:708–9.
22. Sheth S, Colletti PM. Atlas of sodium fluoride PET bone scans: atlas of NaF PET bone scans. *Clin Nucl Med* 2012;**37**:e110–6.
23. Swiętaszczyk C, Prasad V, Baum RP. Intense ^{18}F-fluoride accumulation in liver metastases from a neuroendocrine tumor after peptide receptor radionuclide therapy. *Clin Nucl Med* 2012;**37**:e82–3.
24. Cai L, Chen Y, Huang Z, *et al*. Incidental detection of solitary hepatic metastasis by ^{99m}Tc-MDP and ^{18}F-NaF PET/CT in a patient with osteosarcoma of the tibia. *Clin Nucl Med* 2015;**40**:759–61.
25. Agrawal K, Bhattacharya A, Harisankar CNB, *et al*. F-18 Fluoride uptake in calcified extraosseous metastases from ovarian papillary serous adenocarci- noma. *Clin Nucl Med* 2012;**37**:e22–3.
26. Van Der Gucht A, Galat A, Rosso J, *et al*. [18F]-NaF PET/CT imaging in cardiac amyloidosis. *J Nucl Cardiol* 2016;**23**:846–9.
27. Teo TY, Menda Y, McNeely P, *et al*. Incidental meningioma detected on ^{18}F-fluoride with PET/CT during initial staging for prostate cancer. *Clin Nucl Med* 2015;**40**:596–7.
28. Asmar A, Simonsen L, Svolgaard B, *et al*. Unexpected diffuse ^{18}F-NaF uptake in the lung parenchyma in a patient with severe hypercalcemia due to myelomatosis. *Clin Nucl Med* 2017;**42**:68–9.
29. Dweck MR, Chow MW, Joshi NV, *et al*. Coronary arterial ^{18}F-sodium fluoride uptake: a novel marker of plaque biology. *J Am Coll Cardiol* 2012;**59**:1539–48.
30. Chen L, Chen Y, Huang Z, *et al*. Intense ^{99m}Tc-MDP and ^{18}F-NaF activity in long-standing subcutaneous implants. *Clin Nucl Med* 2016;**41**:812–4.
31. Wong KK, Piert M. Dynamic bone imaging with ^{99m}Tc-labeled diphosphonates and ^{18}F-NaF: mechanisms and applications. *J Nucl Med* 2013;**54**:590–9.
32. Joshi NV, Vesey AT, Williams MC, *et al*. ^{18}F-fluoride positron emission tomography for identification of ruptured and high-risk coronary atherosclerotic plaques: a prospective clinical trial. *Lancet* 2014;**383**:705–13.
33. Derlin T, Wisotzki C, Richter U, *et al*. *In vivo* imaging of mineral deposition in carotid plaque using ^{18}F-sodium fluoride PET/CT: correlation with atherogenic risk factors. *J Nucl Med* 2011;**52**:362–8.
34. Derlin T, Richter U, Bannas P, *et al*. Feasibility of ^{18}F-sodium uoride PET/CT for imaging of atherosclerotic plaque. *J Nucl Med* 2010;**51**:862–5.
35. Zou Y, Chen Y, Huang Z, *et al*. Elevated ^{99m}Tc-MDP and ^{18}F-NaF uptake in a bladder stone. *Clin Nucl Med* 2016;**41**:732–3.
36. Nasseri F, Naeini D. Differential diagnosis of a persistent tracer uptake in the paraspinal lumbar area detected by SPET and CT: an ureteral calculus? *Hell J Nucl Med* 2009;**12**:74–5.
37. Onur D, Seymen H, Ihsan K, *et al*. Bone tracer uptake in urinary bladder stones. *Clin Nucl Med* 2003;**28**:337–9.
38. Styles CB, Niekrash RE. Bone tracer uptake in a ureteric calculus. *Australas Radiol* 1998;**42**:83–5.
39. Subbiah V, Anderson P, Rohren E. Alpha emitter radium 223 in high-risk osteosarcoma: first clinical evidence of response and blood–brain barrier penetration. *JAMA Oncol* 2015 May;**1**:253–5.
40. Jones RP, Iagaru A. ^{18}F NaF brain metastasis uptake in a patient with melanoma. *Clin Nucl Med* 2014;**39**:e448–50.
41. Thenkondar A, Jafari L, Sooriash R. ^{18}F-NaF PET Demonstrating unusual focal tracer activity in the brain. *Clin Nucl Med* 2017;**42**:127–8.
42. Li Y, Berenji G, Shaba W, *et al*. Association of vascular fluoride uptake with vascular calcification and coronary artery disease. *Nucl Med Commun* 2012;**33**:14–20.
43. Adamson PD, Vesey AT, Joshi NV, *et al*. Salt in the wound: (18)F-fluoride positron emission tomography for identification of vulnerable coronary plaques. *Cardiovasc Diagn Ther* 2015;**5**:150–5.
44. Aktas GE, Sarıkaya A, Can N, *et al*. Microcalcified hepatic metastases incidentally detected on F-18 NaF PET/CT in a patient with prostate cancer. *Nucl Med Mol Imag* 2017;**51**:364–7.
45. Basu S, Kembhavi S. Serendipitous observation of hepatic metastases on (18)F-fluoride PET in a patient with infiltrating ductal carcinoma of breast: correlation with contrast enhanced CT. *Clin Nucl Med* 2012;**37**:1176–8.
46. Li Y, Tafti B, Shaba W, *et al*. Extraosseus uptake of ^{18}F sodium fluoride in the primary malignancy and cerebral metastasis in a case of non-small cell lung cancer. *Clin Nucl Med* 2011;**36**:609–11.
47. Jackson T, Mosci C, von Eyben R. Combined ^{18}F-NaF and ^{18}F-FDG PET/CT in the evaluation of sarcoma patients. *Clin Nucl Med* 2015;**40**:720–4.
48. Zhang S, Chen Y, Huang Z, *et al*. Significant ^{99m}Tc-MDP but unimpressive ^{18}F-NaF gastric activity in a patient with multiple myeloma. *Clin Nucl Med* 2016;**41**:740–2.
49. Hawkins AS, Howard BA. Unusual soft tissue uptake of F-18 sodium fluoride in three patients undergoing F-18 NaF PET/CT bone scans for prostate cancer. *Nucl Med Mol Imag* 2017;**51**:274–6.
50. Shao F, Zou Y, Cai L, *et al*. Unexpected detection of urinary bladder cancer on dual phase ^{18}F-NaF PET/CT in a patient with back pain. *Clin Nucl Med* 2016;**41**:902–4.